MECSOL 2022 - Proceedings of the 8th International Symposium on Solid Mechanics
M.L. Bittencourt, J. Labaki, L.C.M. Vieira Jr. and E. Mesquita (Editors), Campinas SP, Brazil, October 17th to 19th, 2022

Temperature Compensation Strategies for SHM based on Electromechanical Impedance: A Comparative Study

Lorena Lopes Dias[1], Camila Gianini Gonsalez Bueno[1], Kayc Wayhs Lopes [1] and Douglas D. Bueno[1]

[1] GMSINT - Group of Intelligent Materials and Systems, Department of Mechanical Engineering, São Paulo State University (UNESP), School of Engineering of Ilha Solteira, Brasil Avenue, 56 - Ilha Solteira, SP - CEP 15.385-000

Abstract. Different structures are subjected to operational and external effects which can generate structural damage. The structural performance must be carefully designed to avoid failures due to their consequences typically involve economic, social and environmental impacts. Damage detection is then one of the great concerns of the engineers, who have carried out numerous researches to develop techniques in the field of structural health monitoring (SHM). Among different techniques, Electromechanical Impedance (EMI) approach has attracted attention due to its important and promising aspects. However, the sensitivity of this technique is related to environmental conditions fluctuations, which can lead to false diagnoses, and the temperature is one of the most critical factors for EMI technique. In this point of view, several researchers have developed compensation methods in order to minimize the effects caused by temperature variation in impedance curves. In this context, the present article provides a comparative study involving two differenttemperature compensation strategies by employing experimental data measured for an aluminum beam on three different conditions: i) without damage, ii) with a damage characterized by an addition of small mass and iii) another one by an introduced mechanical cut on the beam. The results obtained indicate that those two techniques investigated are able to minimize the temperature effect in the studied system, and one of them presents a better performance to reduce false alarms in damage detections using the eletromechanical impedance technique.
Keywords: *Structural health monitoring, Electromechanical impedance, Comparative Study, Temperature Compensation Techniques, Aluminum beam.*

INTRODUCTION

Structural health monitoring (SHM) is the observation and analysis of different engineering structures to monitor any changes in material and geometric properties that could be an indication of possible failure. To identify these damages or malfunctions, sensors are usually employed to obtain damage-sensitive information from the structural system over time. The obtained measurements are post-processed to determine the system structural state (Farrar et al., 2005; Worden and Dulieu-Barton, 2004).

Electromechanical Impedance (EMI) is used in SHM. This technique typically comprises the use of piezoelectric transducers (PZT) that act as both actuator and sensor, i.e., it excites the monitored structure and measures its response (Wang et al., 2014). Its approach basically consists on measuring EMI for the non-damage condition, known as baseline signal, and then, this data is compared with other EMI signals obtained for unknown structural conditions (Bhalla and Soh, 2004; Sun et al., 1995).

Despite several studies demonstrating the feasibility of applying EMI technique, practical problems have prevented its efficient and reliable use in real structures, with temperature effects being cited as one of the most critical and challenging (Baptista et al., 2014). Electromechanical impedance signals are directly affected by changes in properties of structure and piezoelectric transducers. Consequently, temperature acts as a key factor for the performance of an SHM system via impedance, since it is responsible for altering materials properties. Therefore, several researchers have sought ways to neutralize the temperature effects on EMI curves through strategies known as compensation techniques. Among these, Park et al. (1999) compensate for frequency and magnitude shifts using a modified metric. Koo et al. (2009) determine the effective frequency shift (EFS) to compensate for temperature effects by maximizing the cross-correlation coefficient (C_C) between baseline and unknown impedance signatures. Among many other researchers who investigate different strategies in order to contribute to the knowledge formation and future use of this technique in real structures (Baptista et al. (2014); Grisso and Inman, 2010; Lim et al., 2011; Sepehry et al., 2011).

In this context, this paper introduces a comparative study by investigating the feasibility of two different temperature compensation techniques proposed by Park et al. (1999) and Koo et al. (2009) to reduce the temperature effects on the EMI curves. Experimental data are measured and analyzed for an aluminum beam, for which the local temperature range

corresponds to -10°C to 80°C. In this structure, two different types of damage are considered, i.e., a local small mass addition and mass/stiffness reduction by an introduced mechanical cut. Each one of those techniques are computationally implemented using an algorithm written in Python® software. It is verified the effectiveness of each one of the techniques for the structural conditions with and without damages. The results demonstrate that the approach proposed by Park et al. (1999) is more interesting for this type of damage detection.

METHODOLOGY

Electromechanical Impedance

Electromechanical Impedance technique consists of using one or more piezoelectric transducers (PZT) as sensor(s) and actuator(s). These devices are responsible for the coupling between structure's mechanical impedance and PZT's electrical impedance, from which the monitoring of structure is carried out (Na and Baek, 2018).

The admittance $Y_{em}(\omega)$, represented in Eq. (1), was introduced by Liang et al. (1993); and its inverse corresponds to the electromechanical impedance $Z_{em}(\omega)$. This equation shows how the structure impedance $Z(\omega)$ and the impedance of a piezoelectric transducer, $Z_A(\omega)$, relate to each other to define the electromechanical impedance.

$$Y_{em}(\omega) = j\omega \frac{b_a L_a}{h_a} \left[\bar{\epsilon}_{33}^{T} - \frac{Z(\omega)}{Z_A(\omega) + Z(\omega)} d_{31} \bar{Y}_{11}^{E} \right] \tag{1}$$

where L_a, b_a and h_a are the length, width and thickness of the PZT, respectively. $\bar{\epsilon}_{33}^{T}$ is the dielectric constant of the PZT in the 3-3 direction (z) under a constant voltage, d_{31} is the piezoelectric constant, $\bar{Y}_{11}^{E}$ is the complex elastic modulus of the PZT in the 1-1 direction (x) under a constant electric field; and $j = \sqrt{-1}$ is the pure imaginary number (Liang et al., 1996).

Experimental Setup

The experiment consisted of collecting impedance signals from an aluminum beam containing a PSI-5H4E piezoelectric patch from Piezo Systems® attached to its surface. Figure 1 shows a schematic of the experimental setup utilized. It was used a National Instruments® board, model NI-USB 6211 (16 bits); a laptop containing the software with the impedance analyzer developed by Baptista and Filho (2009) in LabView® environment; and a protoboard containing a resistance of 10 $k\Omega$, which acts as an auxiliary circuit.The experiment was carried out with the aluminum beam in free-free condition, which was inserted into a Thermotron® thermal chamber S-Series. Geometric characteristics of the beam and the piezoelectric transducer are presented in Tab. 1.

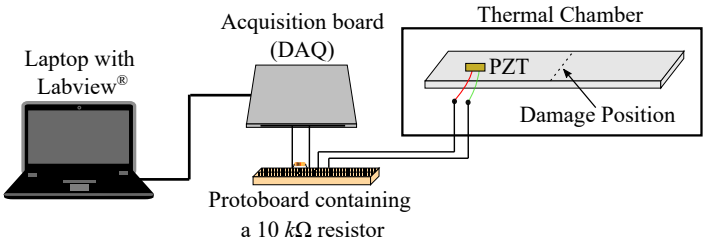

Figure 1 – Experimental setup.

Table 1 – Geometrical characteristics of the beam and the PZT.

Properties	Beam	PZT
Length (mm)	500	10
Width (mm)	13	5
Thickness (mm)	3	0.7

The signals were measured in a temperature range from -10°C to 80°C, which correspond to a large portion of the structures in operation. It was utilized a step of 2°C and 5°C for the non-damage situation and damaged condition, respectively. In order to excite the structure, it was applied a sinusoidal frequency sweep with an amplitude of ±5 V in a

frequency range of 0 to 125 kHz. In addition, two types of damage were considered (both 20 cm from PZT). The first one is the addition of a 4.89 g durepoxy mass (damage 1) and the second one is a 4 mm cut (damage 2).

Selected Data

The selected temperatures for the undamaged signal were: -10°C, 4°C, 24°C, 36°C, 52°C, 64°C, and 80°C, with the impedance signature at 24°C as reference. While the signals for the damaged condition were investigated at temperatures of 5°C, 25°C, 35°C, 50°C, 65°C and 80°C. The frequency range varied from 30 kHz to 45 kHz (15 kHz).

Figures 2 and 3 contain the curves of the real part of the electromechanical impedance of the signals with and without damage at the selected temperatures and frequency range. In all cases, the reference impedance was also plotted to make a visual comparison between the different curves.

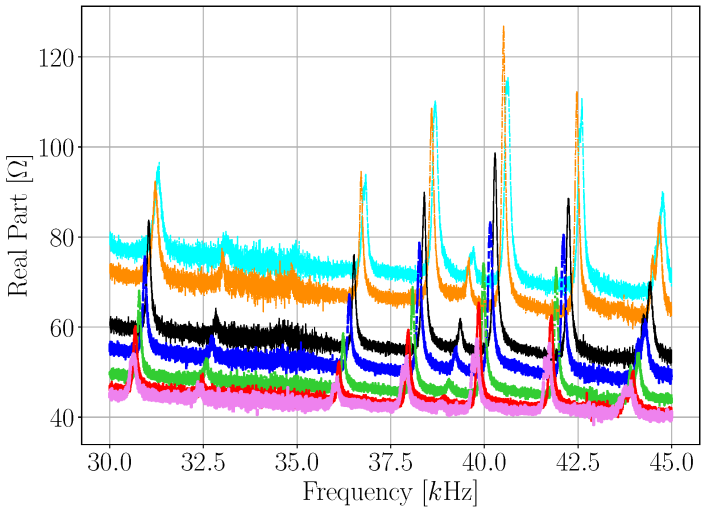

Figure 2 – Real part of the electromechanical impedance (undamaged condition) at different temperatures. Cyan thin dashed line represents -10°C; orange thin dash-dotted line corresponds to 4°C; black thin solid line represents 24°C (reference); blue thick dashed line corresponds to 36°C; green thick dash-dotted line represents 52°C; red thick solid line corresponds to 64°C; solid and very thick violet line represents 80°C.

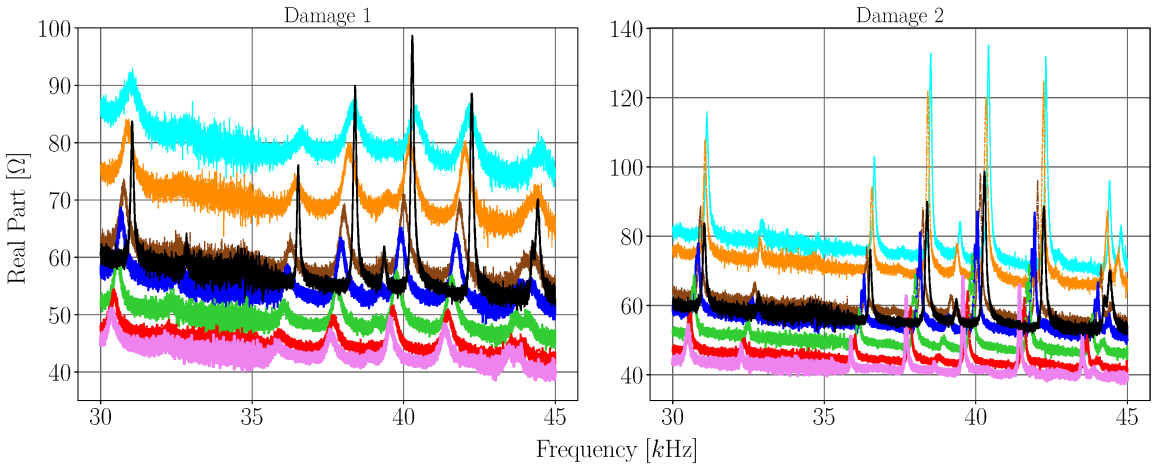

Figure 3 – Real part of the electromechanical impedance (damage 1 and 2) at different temperatures. Cyan thin solid line represents -10°C; orange thin dashed line corresponds to 5°C; brown thin dash-dotted line represents 25°C; blue thick solid line corresponds to 35°C; green thick dashed line represents 50°C; red thick dash-dotted line corresponds to 65°C; solid and very thick violet line represents 80°C; black thin solid line represents 24°C (reference).

Compensation Techniques

Temperature fluctuations cause shifts in frequency (horizontal) and magnitude (vertical) of electromechanical impedance curves, as well as peak smoothing. In view of this, diagnosis can lead to false positives or negatives. Therefore, several researchers sought ways to neutralize the temperature effects on EMI curves through strategies known as compensation techniques. Among they, this paper will study those developed by Park et al. (1999) and Koo et al. (2009).

Park et al. (1999) Technique

Park et al. (1999) develop a technique based on empirical approach in order to minimize the temperature effects on impedance-based SHM method. The procedure to apply the compensation is based on V_a minimization. V_a represents the sum of the real impedance changes squared and is defined by Eq. (2). In this technique, j varies, taking advantage that the variation in impedance is dominated by horizontal shift of impedance peak.

$$V_a = \sum_{i,j=1}^{N} [Re(Z_R(\omega_i)) - Re(Z_D(\omega_j))]^2 \tag{2}$$

where N is the number of frequency points, $Re(Z_R(\omega_i))$ is the real part of the reference impedance (Z_R) at frequency i and $Re(Z_D(\omega_j))$ is the real part of the unknown impedance (Z_D) at frequency j (lagged with respect to i), which is calculated according to Eq. (3). The unknown impedance $Z_D(\omega_j)$ can be generated from the unknown measured impedance according to the following relation:

$$Re(Z_D(\omega_j)) = Re(Z_D(\omega_j)_{medido}) + \delta^S \tag{3}$$

where δ^S is defined as the average difference between reference impedance curve and measured impedance. The values of (j) and δ^S can be found by iteration by shifting the impedance curves to the right, for temperatures above the reference temperature, or to the left, for temperatures below the reference temperature, until the minimum value of V_a is reached. For a better understanding of this technique, the behavior of the impedance curves during the application of Park et al. (1999) technique is presented in the Appendix A.

Koo et al. (2009) Technique

To compensate the impedance variation due to the temperature changes, Koo et al. (2009) determine the effective frequency shift (EFS) by the cross-correlation (C_C) between reference and measured impedance data. The EFS($\tilde{\omega}$) for an unknown impedance Z_D is defined as the shift corresponding to the maximum cross-correlation with the reference impedance Z_R, as shown below:

$$\max_{\tilde{\omega}} C_C = \max_{\tilde{\omega}} \frac{\{1/N \sum_{i=1}^{N} (Z_R(\omega_i) - \bar{Z}_R)(Z_D(\omega_i - \tilde{\omega}) - \bar{Z}_D)\}}{\sigma_{Z_R} \sigma_{Z_D}} \tag{4}$$

where $\bar{Z}_R$ and $\bar{Z}_D$ are the mean values of two impedance signatures of $Z_R(\omega)$ and $Z_D(\omega)$; σ_{Z_R} and σ_{Z_D} are their standard deviations, respectively, and $\tilde{\omega}$ represents the value of EFS during the calculation of the maximum value of C_C. The EFS method may compensate the vertical shifts as well by subtracting the mean values of the original reference signal and the horizontally shifted unknown signal, as shown below:

$$\hat{Z}_D(\omega) = \frac{(Z_D(\omega - \tilde{\omega}) - \bar{Z}_D)}{\sigma_{Z_R} \sigma_{Z_D}} \tag{5}$$

$$\hat{Z}_R(\omega) = \frac{(Z_R(\omega) - \bar{Z}_R)}{{\sigma_{Z_R}}^2} \tag{6}$$

where $\hat{Z}(\omega)$ is the normalized impedance on both axes (amplitude and frequency). Normalization is responsible for changing the signals so that they are all on the same scale, correcting the smoothing of the peaks due to temperature. For a better understanding of this technique, the behavior of the impedance curves during the application of Koo et al. (2009) technique is presented in the Appendix A.

Metric Indexes

Quantitative damage characterization is performed using metric indices. It was used Root Mean Square Deviation (RMSD) and Correlation Coefficient Deviation Metric (CCDM).

RMSD: this index is calculated as presented in Eq. (7) (Park et al., 1999; Koo et al., 2009; Baptista et al., 2014).

$$RMSD = \sum_{i=1}^{N} \sqrt{\frac{[Z_D(\omega_i) - Z_R(\omega_i)]^2}{[Z_R(\omega_i)]^2}} \tag{7}$$

CCDM: presented in Eq. (8), this index is defined as the subtraction between 1 and the cross-correlation coefficient C_C, Eq. (4), given by (Koo et al., 2009; Baptista et al., 2014)

$$CCDM = 1 - C_C \tag{8}$$

RESULTS AND DISCUSSION

The techniques were implemented and the results obtained are shown. Also, the metric indices tendency analysis (RMSD and CCDM) obtained after compensation of EMI curves for each technique is presented. All the results shown below were obtained by using the algorithm implemented in the Python® software.

Analysis of Park et al. (1999) Technique

Figures 4 and 5 contain the curves of the real part of the electromechanical impedance after implementing Park et al. (1999) technique in the three conditions: non-damage, damage 1 (mass addition) and damage 2 (cut).

By using Park et al. (1999) compensation technique, it was possible to observe the correction of both axes (frequency and magnitude). The curves were practically overlapped, demonstrating the effectiveness of this technique to mitigate the temperature effects. Park et al. (1999) technique was able to present a good efficiency even with the signals presenting noise.

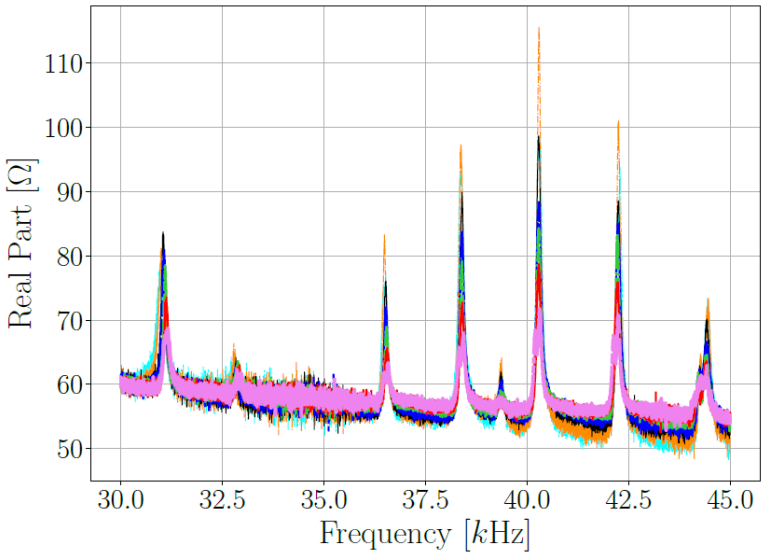

Figure 4 – Real part of EMI (undamaged condition) using Park et al. (1999) compensation technique. Cyan thin dashed line represents -10°C; orange thin dash-dotted line corresponds to 4°C; black thin solid line represents 24°C (reference); blue thick dashed line corresponds to 36°C; green thick dash-dotted line represents 52°C; red thick solid line corresponds to 64°C; solid and very thick violet line represents 80°C.

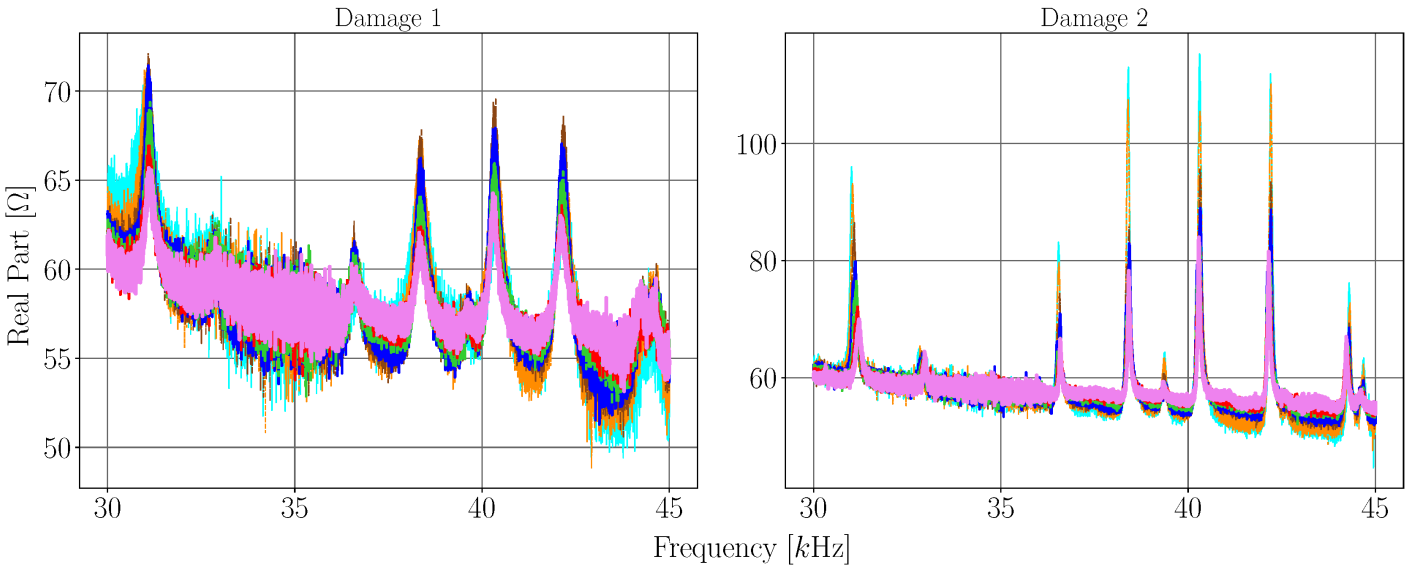

Figure 5 – Real part of EMI (damage 1 and 2) using Park et al. (1999) compensation technique. Cyan thin solid line represents -10°C; orange thin dashed line corresponds to 5°C; brown thin dash-dotted line represents 25°C; blue thick solid line corresponds to 35°C; green thick dashed line represents 50°C; red thick dash-dotted line corresponds to 65°C; solid and very thick violet line represents 80°C.

Analysis of Koo et al. (2009) Technique

Figures 6 and 7 contain the curves of the real part of the normalized electromechanical impedance after implementing Koo et al. (2009) technique in the three conditions: non-damage, damage 1 and 2.

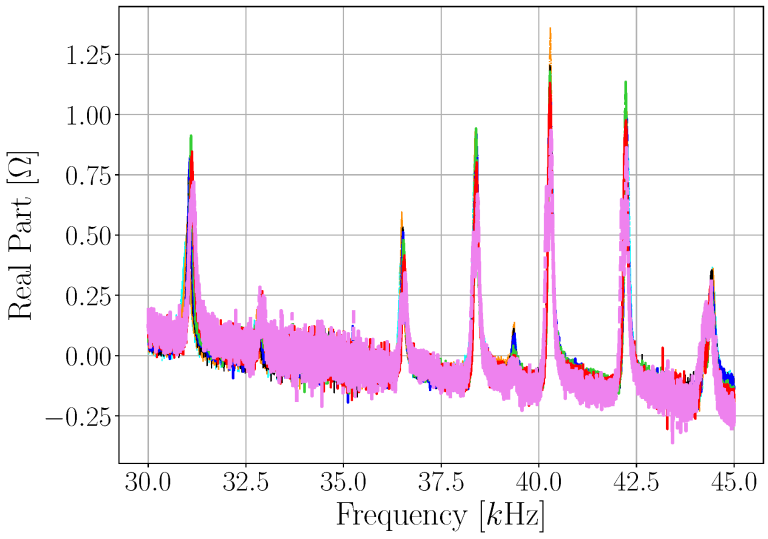

Figure 6 – Real part of EMI (undamaged condition) using Koo et al. (2009) compensation technique. Cyan thin dashed line represents -10°C; orange thin dash-dotted line corresponds to 4°C; black thin solid line represents 24°C (reference); blue thick dashed line corresponds to 36°C; green thick dash-dotted line represents 52°C; red thick solid line corresponds to 64°C; solid and very thick violet line represents 80°C.

The curves after implementing this technique (Figs. 6 and 7) were shifted to the vertical zero axis, as can be seen by comparing them with the original curves (Figs. 2 and 3). Nevertheless, they maintain the same trend and behavior as the original signals in Figs. 2 and 3, except for the peak's amplitude. In this technique, the peak smoothing due to temperature variation is corrected by normalizing the impedance curves, so that all signals are on the same scale, which doesn't occur

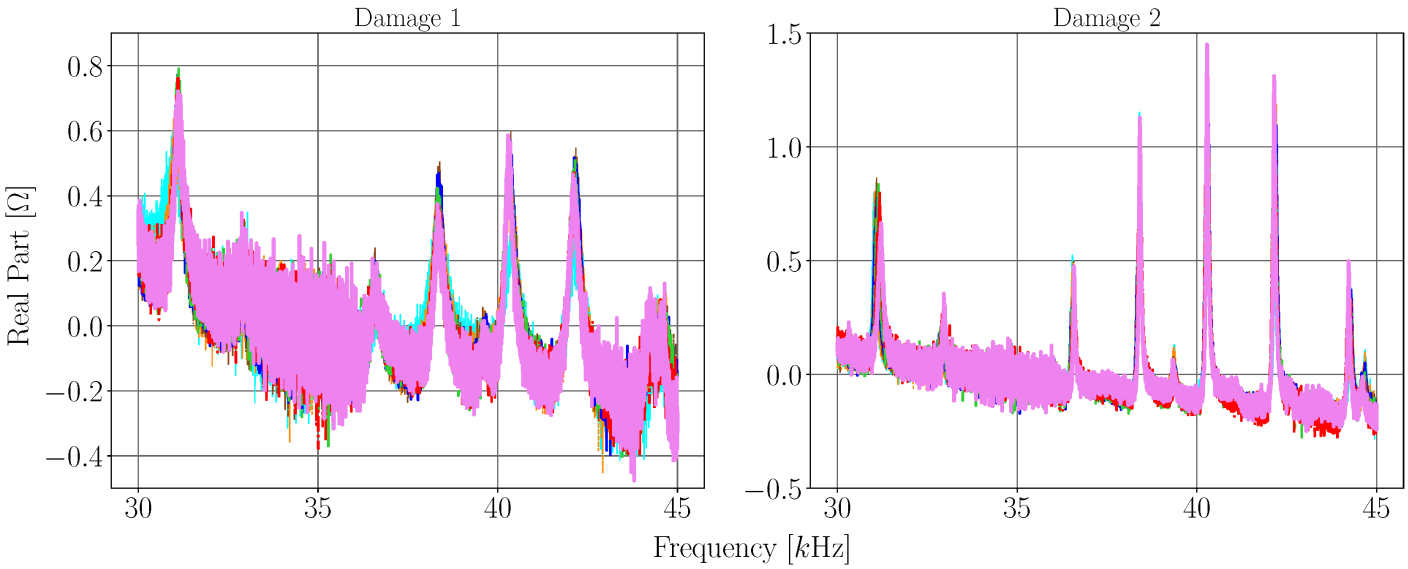

Figure 7 – Real part of EMI (damage 1 and 2) using Koo et al. (2009) compensation technique. Cyan thin solid line represents -10°C; orange thin dashed line corresponds to 5°C; brown thin dash-dotted line represents 25°C; blue thick solid line corresponds to 35°C; green thick dashed line represents 50°C; red thick dash-dotted line corresponds to 65°C; solid and very thick violet line represents 80°C.

for Park et al. (1999) technique. Besides, both axes (amplitude and frequency) are also compensated, so that all the curves are practically overlapping.

Metric Indices Tendency

Figure 8 presents the calculated RMSD and CCDM values for the signals in the undamaged, damage 1 and damage 2 conditions after applying Park et al. (1999) technique. While the metrics obtained for Koo et al. (2009) technique are shown in Fig. 9.

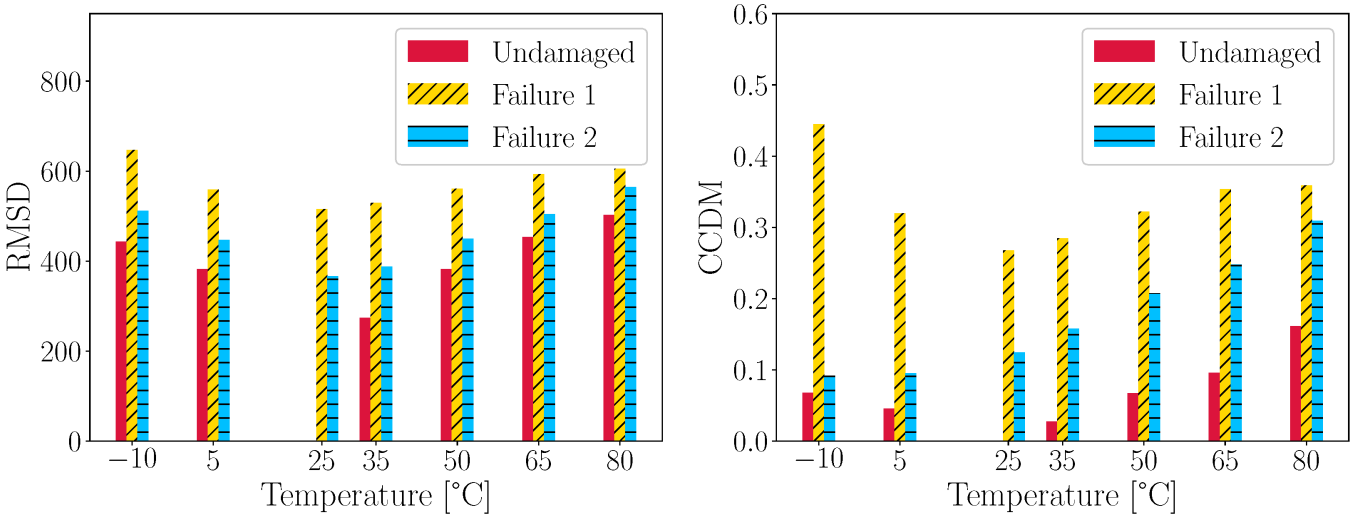

Figure 8 – RMSD and CCDM values of signals compensated by the Park et al. (1999) technique.

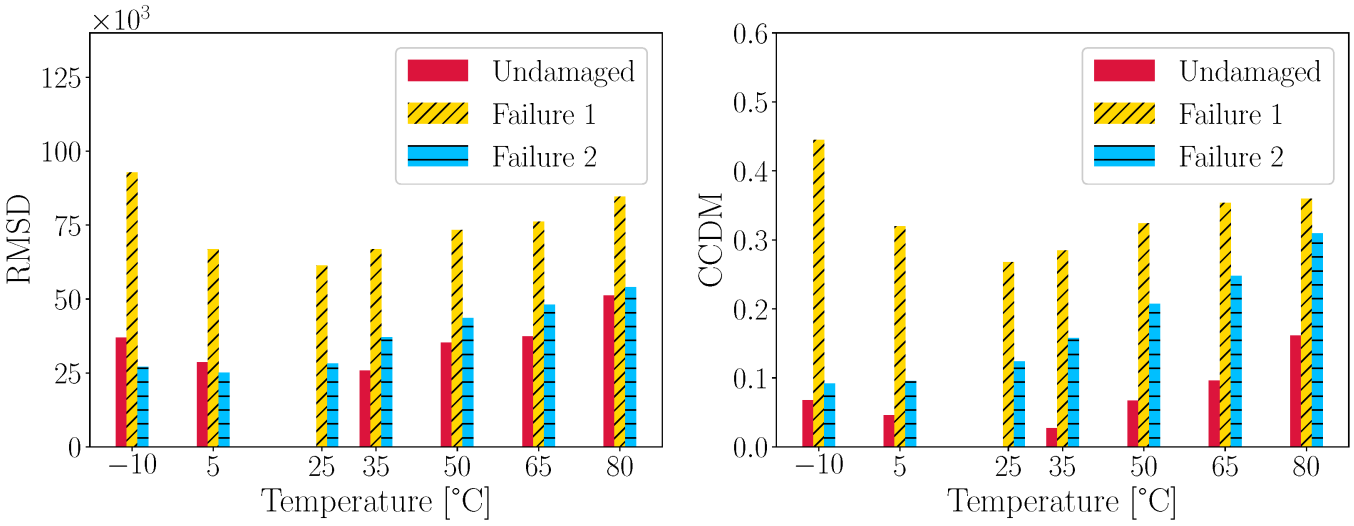

Figure 9 – RMSD and CCDM values of signals compensated by the Koo et al. (2009) technique.

RMSD and CCDM values obtained for damaged condition 1 and 2 remained above the values calculated for the non-damaged condition, demonstrating that even after implementing Park et al. (1999) technique, the quantitative indices can detect the damage.

For Koo et al. (2009) technique, the CCDM index was able to detect damage at all temperatures. However, in the case of RMSD, damage 2 was not detected at temperatures of -10°C and 5°C, while damage 1 was detected at all analyzed temperatures, since it causes a greater structural change.

CONCLUSIONS

This paper aimed to investigate the feasibility of using two different temperature compensation techniques on the electromechanical impedance curves to damage detection in mechanical systems. The compensation of temperature effects are evaluated for an aluminum beam including two different structural conditions, which corresponds to the health structure (i.e., without damage) and the damaged one.

Park et al. (1999) compensation technique is more effective in this present study. It is able to reduce the temperature effects and still detect the presence of damage. On the other hand, Koo et al. (2009) strategy is able to significantly minimize the temperature effects by determining the normalized impedances. However, at temperatures of -10°C and 5°C, the RMSD-based index does not detect the damage type 2 (i.e., the mechanical cut).

In conclusion, for the proposed system, Park et al. (1999) and Koo et al. (2009) techniques are efficient in compensating the temperature effects caused by environmental temperature variations. In particular, Park et al. (1999) technique is the most appropriate to be implemented in structural health monitoring system for this type of structure and damage.

REFERENCES

Baptista, F. G., Budoya, D. E., De Almeida, V. A. D. and Ulson, J. A. C., 2014, "An experimental study on the effect of temperature on piezoelectric sensors for impedance-based structural health monitoring", Sensors, Vol. 14, pp. 1208-1227.

Baptista, F. G. and Filho, J. V., 2009, "A new impedance measurement system for pzt based structural health monitoring", IEEE Transaction on Instrumentation and Measurement, Vol. 58, No. 10, pp. 3602-3608.

Bhalla, S. and Soh, C. K., 2004, "Electromechanical impedance modeling for adhesively bonded piezo-transducers", Journal of Intelligent Material Systems and Structures, Vol. 15, No. 12, pp. 955-972.

Farrar, C.R., Lieven, N.A.J. and Bement, M.T., 2005. "Damage Prognosis for Aerospace, Civil and Mechanical Systems", Wiley, 1st edition.

Grisso, B. L. and Inman, D. J., 2010, "Temperature corrected sensor diagnostics for impedance-based shm", Journal of

Sound and Vibration, Vol. 329, No. 12, pp. 2323-2336.

Koo, K. Y., Park, S., Lee, J. J. and Yun, C. B., 2009, "Automated impedance-based structural health monitoring incorporating effective frequency shift for compensating temperature effects", Journal of Intelligent Material Systems and Structures, Vol. 20, No. 4, pp. 367-377.

Liang, C., Sun, F. P. and Rogers, C. A., 1993, "Coupled electromechanical analysis of piezoelectric ceramic actuator-driven systems: determination of the actuator power consumption and system energy transfer", Smart Structures and Materials, https://doi.org/10.1117/12.152767.

Liang, C., Sun, F. P. and Rogers, C. A., 1996, "Electro-mechanical impedance modeling of active material systems", Smart Materials and Structures, Vol. 5, No. 2, pp. 171-186.

Lim, H. J., Kim, M. K., Sohn, H. and Park, C. Y., 2011, "Impedance based damage detection under varying temperature and loading conditions", Ndt and E International, Vol. 44, pp. 740-750.

Lopes, K. W., 2018, "Detecção de falhas experimentais em estruturas mecânicas utilizando sistemas imunológicos artificiais", Fundação de Amparo à Pesquisa do Estado de São Paulo (FAPESP). São Paulo, Brasil.

Na, W. S. and Baek, J., 2018, "A review of the piezoelectric electromechanical impedance based structural health monitoring technique for engineering structures", Sensors,Vol. 18, No. 5.

Park, G., Kabeya, K., Cudney, H. H. and Inman, D. J., 1999, "Impedance-based structural health monitoring for temperature varying applications", JSME International Journal Series A, Vol. 42, No. 2, pp. 249-258.

Sepehry, N., Shamshirsaz, M. and Abdollahi, F., 2011, "Temperature variation effect compensation in impedance-based structural health monitoring using neural networks", Journal of Intelligent Material Systems and Structures, Vol. 22, pp. 1975-1982.

Sun, F. P., Chaudhry, Z., Liang, C. and Rogers, C. A., 1995, "Truss structure integrity identification using pzt sensor-actuator", Journal of Intelligent Material Systems and Structures,Vol. 6, No. 1, pp. 134-139.

Wang, D., Song, H. and Zhu, H., 2014, "Electromechanical impedance analysis on piezoelectric smart beam with a crack based on spectral element method", Mathematical Problems in Engineering, pp. 13.

Worden, K. and Dulieu-Barton, J.M., 2004. "An overview of intelligent fault detection in systems and structures", Structural Health Monitoring, Vol. 3, No. 1, pp. 85–98.

RESPONSIBILITY NOTICE

The author(s) is (are) the only party(ies) responsible for the printed material included in this paper.

APPENDIX A

This appendix shows the behavior of the impedance curves when applying Park et al. (1999) and Koo et al. (2009) compensation techniques.

The behavior of electromechanical impedance curves when applying Park et al. (1999) technique can be seen in Fig. 10, which contains the real part of the EMI obtained for an aluminum beam in the undamaged condition at 10°C and 30°C (reference) in 4 different stages (iterations). After 1 iteration, it is already possible to observe the vertical axis compensation, by summing δ^S to the unknown signal. Moreover, this variable presents a low variation even after multiple iterations. This occurs because δ^S is calculated as the difference between Z_R and measured signal shifted only horizontally, in order to employ its updated value in each iteration.

Figure 11 shows the behavior of the electromechanical impedance curves with the application of Koo et al. (2009) technique. The same signals used to exemplify Park et al. (1999) technique are employed here. The impedance signal is shifted in each iteration in order to obtain the maximum value of C_C. The values of $\bar{Z}_D$ and σ_{Z_D} suffer little variation, while C_C increases. Furthermore, vertical axis compensation only occurs when applying Eqs. (5) and (6) to determine the normalized impedance.

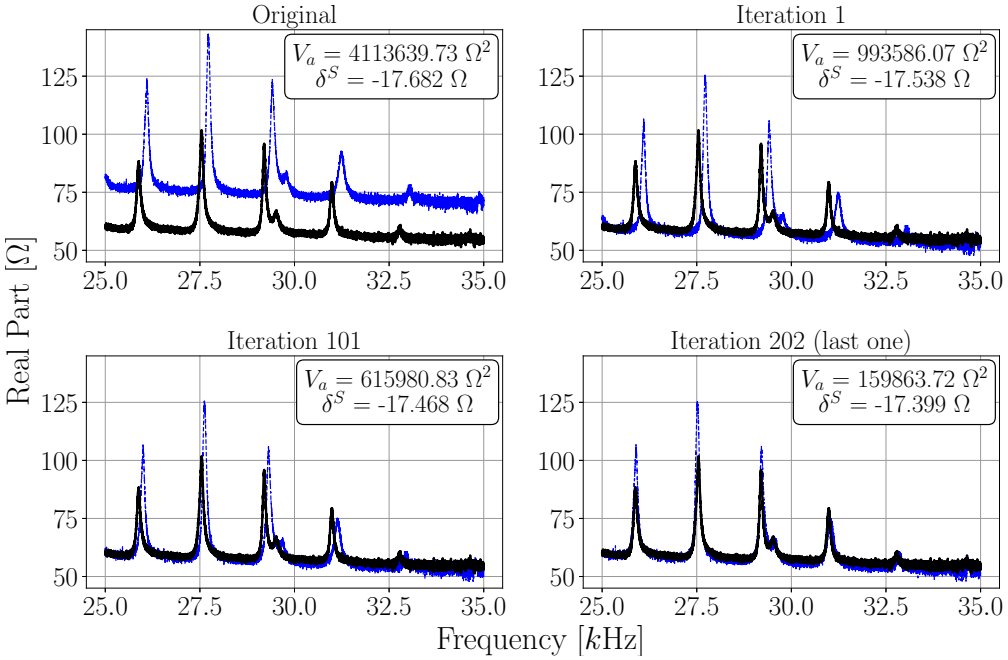

Figure 10 – Real part of electromechanical impedance at different iterations of Park et al. (1999) technique for the reference (black continuous line) and the unknown (blue dashed line) signal.

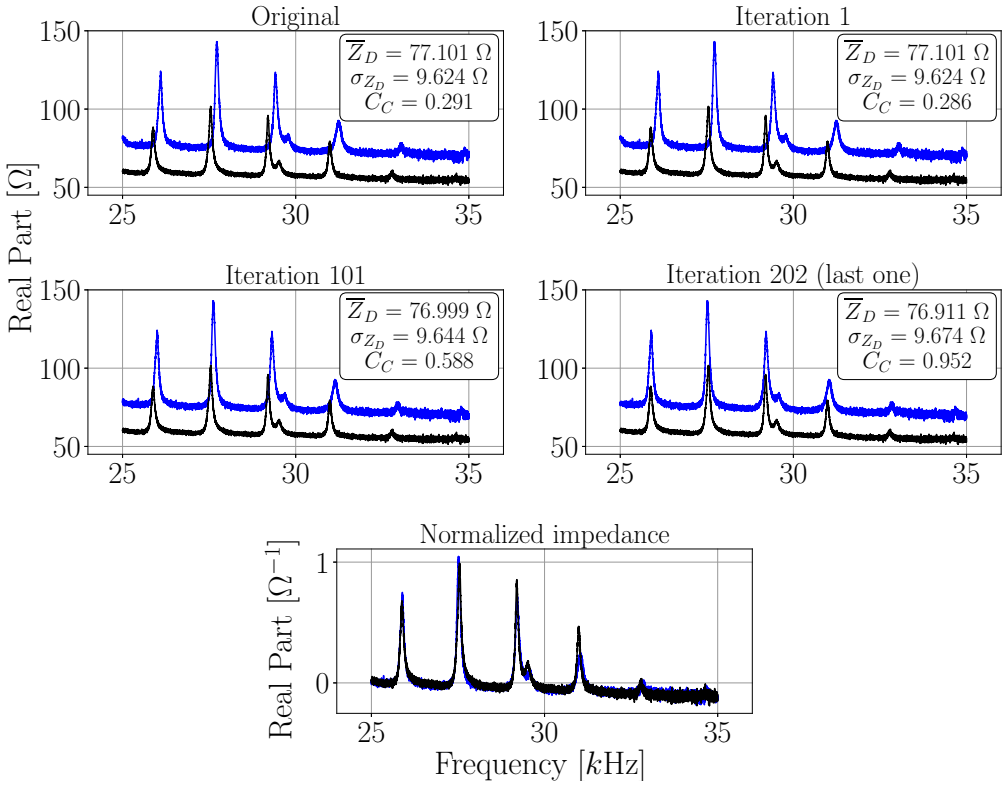

Figure 11 – Real part of electromechanical impedance at different iterations of Koo et al. (2009) technique for the reference (black continuous line) and the unknown (blue dashed line) signal.